Revue des sciences de l’eau
Journal of Water Science

Arsenic(v) removal from aqueous solutions using ferromagnetic activated carbon: equilibrium and kinetic studies
Élimination de l’arsenic(V) en solutions aqueuses par le charbon actif ferromagnétique : étude de l’équilibre et de la cinétique

Yacouba Sanou, Nguyen Thi Thanh Phuong, Samuel Pare et Nguyen Van Phuoc

Volume 32, numéro 2, 2019

Received 5 June 2019, accepted on 8 June 2019

URI : https://id.erudit.org/iderudit/1065206ar
DOI : https://doi.org/10.7202/1065206ar

Aller au sommaire du numéro

Éditeur(s)

Université du Québec - INRS-Eau, Terre et Environnement (INRS-ETE)

ISSN

1718-8598 (numérique)

Découvrir la revue

Citer cet article

Sanou, Y., Phuong, N. T. T., Pare, S. & Phuoc, N. V. (2019). Arsenic(v) removal from aqueous solutions using ferromagnetic activated carbon: equilibrium and kinetic studies. *Revue des sciences de l’eau / Journal of Water Science*, *32*(2), 179–192. https://doi.org/10.7202/1065206ar

Résumé de l'article

La pollution des eaux par l’arsenic est un des problèmes globaux qui entravent l’approvisionnement en eau potable au Burkina Faso, principalement en milieu rural. Pour pallier cette pollution, du charbon actif ferromagnétique a été préparé par activation chimique à partir de balles de riz et de chlorure de fer hexahydraté pour être utilisé comme adsorbant dans le traitement de l’arsenic. La caractérisation de ce charbon par des techniques analytiques a révélé un charbon microporeux avec une surface spécifique de 150 $m^2 \cdot g^{-1}$ et une propriété ferromagnétique. Ce travail a pour but d’évaluer les conditions d’équilibre de l’élimination de l’As(V) et la capacité d’adsorption du charbon actif. Des expériences en mode batch ont été réalisées pour évaluer la performance de ce charbon dans l’élimination de l’arsenic sous différentes conditions ainsi que pour étudier la cinétique du processus. Les résultats ont montré une augmentation de l’élimination de l’As(V) avec le temps de contact et la saturation du charbon a été obtenue au bout de 60 min de contact. L’augmentation de la concentration initiale en As(V) a entrainé une augmentation de la capacité d’adsorption qui est passé de 0,12 à 3,66 $\mu g \cdot g^{-1}$. L’augmentation du pH entre 3 et 11 a révélé une variation du taux d’élimination de l’As(V) avec un maximum à pH = 7 correspondant à une capacité d’adsorption de 153 $\mu g \cdot g^{-1}$. L’adsorption en monocouche, suivie d’un échange anionique, constitue le mécanisme de l’élimination de l’As(V) par le charbon. La cinétique du processus est de pseudo-second ordre.

ARSENIC(V) REMOVAL FROM AQUEOUS SOLUTIONS USING FERROMAGNETIC ACTIVATED CARBON: EQUILIBRIUM AND KINETIC STUDIES

Élimination de l'arsenic(V) en solutions aqueuses par le charbon actif ferromagnétique : étude de l'équilibre et de la cinétique

Yacouba SANOU[1], Nguyen Thi Thanh PHUONG[2], Samuel PARE[1], Nguyen Van PHUOC[2]*

[1]Laboratory of Analytical, Environmental and Bio-Organic Chemistry (LCAEBiO), Chemistry Department, University Joseph KI-ZERBO, 03 BP 7021 Ouagadougou 03, Burkina Faso
[2]Institute for Environment and Resources (IER/HCMC), Vietnam National University, 142 To Hien Thanh Street, District 10, Ho Chi Minh City, Vietnam

Received 5 June 2019, accepted on 8 June 2019

ABSTRACT

Arsenic pollution is one of the global issues which affect the drinking water supply in Burkina Faso, mainly in rural areas. To mitigate this water pollution, ferromagnetic activated carbon (FAC) has been prepared by chemical activation using rice husk and iron chloride solution to be used as an adsorbent of arsenic. Characterization with some analytical techniques revealed this carbon is microporous with a specific surface area of 150 $m^2 \cdot g^{-1}$ and ferromagnetic properties. This work aims to evaluate the equilibrium conditions of As(V) removal and the adsorption capacity of FAC. Batch experiments were undertaken to evaluate the performance of FAC for arsenic removal under various operating conditions and the mechanism of the removal process. Results showed an increase of the removal percentage with the increase of the contact time, indicating a saturation during 60 min. The removal of As(V) is influenced by the increase of the initial arsenic concentration causing an increase of the adsorption capacity of FAC. The increase of pH showed a variation of the removal percentage indicating a maximum removal at pH 7 which corresponds to an adsorption capacity of 153 $\mu g \cdot g^{-1}$. Both monolayer adsorption and ion exchange constitute the mechanism of removal of As(V) using FAC. The kinetics of the process is described by a pseudo-second order model.

Key words: arsenic removal, chemical activation, ferromagnetic activated carbon, water.

RÉSUMÉ

La pollution des eaux par l'arsenic est un des problèmes globaux qui entravent l'approvisionnement en eau potable au Burkina Faso, principalement en milieu rural. Pour pallier cette pollution, du charbon actif ferromagnétique a été préparé par activation chimique à partir de balles de riz et de chlorure de fer hexahydraté pour être utilisé comme

---

[*] Corresponding author:
Phone: (+226) 72191530
Email: prosper_yacson@yahoo.fr

ISSN : 1718-8598

adsorbant dans le traitement de l'arsenic. La caractérisation de ce charbon par des techniques analytiques a révélé un charbon microporeux avec une surface spécifique de 150 $m^2 \cdot g^{-1}$ et une propriété ferromagnétique. Ce travail a pour but d'évaluer les conditions d'équilibre de l'élimination de l'As(V) et la capacité d'adsorption du charbon actif. Des expériences en mode batch ont été réalisées pour évaluer la performance de ce charbon dans l'élimination de l'arsenic sous différentes conditions ainsi que pour étudier la cinétique du processus. Les résultats ont montré une augmentation de l'élimination de l'As(V) avec le temps de contact et la saturation du charbon a été obtenue au bout de 60 min de contact. L'augmentation de la concentration initiale en As(V) a entrainé une augmentation de la capacité d'adsorption qui est passé de 0,12 à 3,66 $\mu g \cdot g^{-1}$. L'augmentation du pH entre 3 et 11 a révélé une variation du taux d'élimination de l'As(V) avec un maximum à pH = 7 correspondant à une capacité d'adsorption de 153 $\mu g \cdot g^{-1}$. L'adsorption en monocouche, suivie d'un échange anionique, constitue le mécanisme de l'élimination de l'As(V) par le charbon. La cinétique du processus est de pseudo-second ordre.

Mots-clés : élimination d'arsenic, activation chimique, charbon actif ferromagnétique, eau.

1. INTRODUCTION

Drinking water supply is one of the most important challenges of African countries, mainly in Sub-Sahara Africa. Water resources are facing many challenges including the increasing demand, pollution, scarcity, climate changes, etc. The presence of toxic trace metals in water, including lead, mercury and arsenic, may impact human health if they occur above World Health Organization (WHO) guidelines for drinking water. According to the WHO, 80% of diseases (malaria, onchocerciasis, gastro-enteritis, etc.) affecting the world's population are transmitted by water (DESJARDINS, 1997). Arsenic contamination in groundwater for drinking purposes has become a worldwide problem and a serious environmental challenge in the world (MEROLA *et al.*, 2015; KNUDSEN *et al.*, 2005; SHANKAR and SHANKER, 2014). The toxicity of arsenic on humans depends on its chemical forms: both inorganic and organic trivalent arsenicals are more potent toxic than pentavalent forms (HUGHES, 2002). Inorganic arsenic is present in natural water in its two predominant oxidation states: As(III) and As(V) with arsenite more mobile and 60 times more toxic than arsenate (MAJI *et al.*, 2007). Out of the trace elements occurring in the groundwaters of northern Burkina Faso, arsenic has the greatest impact on human health. Medical problems such as skin lesions and cancer are widely known to occur as a consequence of chronic arsenic intake in Northern Burkina Faso (SOME *et al.*, 2012). A previous study in Yatenga Province (North Burkina Faso) showed high arsenic concentrations in tube-wells, which are used by 87% of villagers. The first recognized consequences from chronic exposure to arsenic are melanosis, a skin disorder of hyperpigmentation or keratosis where the skin becomes rough and dry with skin papules (SOME *et al.*, 2012). Arsenic pollution in this area was due to arsenopyrite species in the bedrock (SMEDLEY *et al.*, 2007). High arsenic concentrations in groundwaters have caused the closing of some wells in Lilgomde and Tanili villages in Burkina Faso. Arsenic contamination in groundwater has also become a major environmental concern in Vietnam (BERG *et al.*, 2001). The presence of arsenic in groundwaters of Dong Thap Province (Vietnam) with arsenic concentrations ranging from 0.5 to 978 $\mu g \cdot L^{-1}$ caused skin rashes, breathing problems, general tiredness, chronic diarrheas, etc. (MEROLA *et al.*, 2015).

Technologies including precipitation/co-precipitation, ion exchange, membrane filtration, and adsorption have been developed to remove arsenic from drinking water (USEPA, 2001). Previous work showed that granular ferric hydroxide (GFH) could be successfully used as adsorbents in As(V) removal (SANOU *et al.*, 2016a). However, the high cost of GFH limits its use in developing countries such as Burkina Faso. In addition, investigation on natural laterite from Vietnam demonstrated successful removal of arsenic from water (SANOU *et al.*, 2016a). Many studies have been focused on the production of iron-coated materials and their use as adsorbent in arsenic removal (MAHMOOD *et al.*, 2018a; ANSONE *et al.*, 2012; DIN *et al.*, 2017). Among them, limited research has concerned the use of agricultural wastes/by-products greatly available in Sub-Saharan Africa. In this regard, activated carbons are prepared in Burkina Faso from local biomass and lignocellulosic materials for water and wastewater treatment (SANOU *et al.*, 2016b; GUEYE, 2015). Preliminary study using ferromagnetic activated carbon (FAC) as an adsorbent of arsenic in column experiments was promising (SANOU *et al.*, 2017). However, the mechanism of the process and the microstructure of FAC have not been studied. Therefore, this present work aims to investigate the efficiency of FAC in As(V) removal using batch experiments under various conditions. The kinetics of the process will be studied in order to explain the mechanism of As(V) removal. In addition, the global chemical composition of FAC, the microstructure and the surface area will be determined using analytical methods.

2. MATERIAL AND METHODS

2.1 Preparation of ferromagnetic activated carbon (FAC)

Rice husk was obtained from rice fields at Koubri Village (12°10'3" N, 1°21'20" W) in Burkina Faso. Ferromagnetic activated carbon was previously prepared through chemical activation (SANOU *et al.*, 2016b). This method is a modification of the one used by THAJEEL *et al.* (2013).

2.2 Characterization of FAC

Brunauer-Emmett-Teller (BET) experiments were used to determine the surface area of carbon using an analyzer at liquid nitrogen temperature. Elemental composition and microstructure of carbon were analyzed with energy dispersive spectroscopy (EDS) and scanning electron microscopy (SEM), respectively using a JED-2300, 7410F microscope coupled to an EDS detector. Fourier transform-infrared spectra of carbon were recorded to detect the surface functional groups using an infrared spectrophotometer (Tensor 27, Bruker, Germany) operating in the range of 4 000-400 cm^{-1} and employing a potassium bromide pellet (KBr). X-rays diffraction of FAC was carried out using a diffractometer (PW-1130, Philips) with the monochromatic radiation $K\alpha_1$ of copper (1.5406 Å).

The index of iodine (I_2) characterizing the microporous structure and the index of methylene blue (MB), considered an indicator of the mesopororosity, were previously determined (SANOU *et al.*, 2017).

2.3 Preparation of As(V) solutions

As(V) solutions were prepared by the dilution of a H_3AsO_4 standard solution (1 000 mg·L^{-1}) in doubly distilled water. Solutions with concentrations ranging from 200 to 1 000 $\mu\text{g·L}^{-1}$ were used in the following experiments. The arsenic (V) standard solution was commercially obtained from chemical stores.

2.4 Arsenic removal experiments

2.4.1 Equilibrium study

Batch experiments were carried out for arsenic removal in aqueous solutions with ferromagnetic activated carbon. Solutions of 25 mL containing a known arsenic concentration were stirred in 50 mL Erlenmeyer flasks at 400 rpm with 0.1 g of carbon and at pH values ranging from 3 to 11 at 26 ± 2°C. The effect of the initial arsenic concentration on the arsenic removal percentage was studied between 200 and 800 $\mu\text{g As·L}^{-1}$ using 0.1 g of FAC in 25 mL of solution with pH 7, 60 min of contact and 26 ± 2 °C at 400 rpm.

After filtration of the mixture using a Whatman filter (0.1 mm), the arsenic concentration was analyzed using the method of hydride generation-atomic absorption spectrophotometer (HG-AAS) at a wavelength of 193.7 nm with an electrode discharge lamp (EDL). The spectrometer was calibrated by using As(V) standard solutions with concentrations ranging from 2 to 20 $\mu\text{g·L}^{-1}$. The minimum limit of detection was 1 $\mu\text{g·L}^{-1}$. Each experiment was carried out three times and the average value was calculated and used in the figures.

2.4.2 Mechanism: kinetics and isotherm studies

The contact time needed for saturation was determined by varying the contact time from 5 to 120 min at 4 000 rpm with 0.1 g of FAC, pH 7, T = 26 ± 2°C and 25 mL of solution containing initially an arsenic concentration of 1 000 $\mu\text{g·L}^{-1}$.

The final concentration and its corresponding adsorption capacity were used to apply the kinetic models of pseudo-first order and pseudo-second order. In addition, the model of WEBER and MORRIS (1963) describing the interaparticle diffusion was applied in order to determine the controlling step of the adsorption kinetics.

Experimental data (final concentration and adsorption capacity) obtained from the study of initial arsenic concentration were used to model different isotherms (Langmuir, Freundlich and Dubinin-Radushkevich).

2.4.3 Calculations

The percentage of arsenic removed was calculated as follows:

$$As(\%) = \left(\frac{C_0 - C_e}{C_0}\right)100 \qquad (1)$$

where C_0 and C_e represent initial and final concentrations of arsenic in solution ($\mu\text{g·L}^{-1}$), respectively.

The adsorption capacity (Q_e) of FAC expressed in $\mu\text{g·g}^{-1}$ was obtained from following relation:

$$Q_e = \left(\frac{C_0 - C_e}{m}\right)V \qquad (2)$$

where V represents the volume of the solution (L) and m is the weight or mass of adsorbent.

3. RESULTS AND DISCUSSION

3.1 Physico-chemical characteristics of FAC

Some parameters such as pH at zero point charge (pH_{ZPC}), surface area, moisture content and bulk density are listed in table 1. We noticed a high BET surface area of FAC compared to activated carbons prepared from the same rice husk (SANOU *et al.*, 2016b). In addition, the higher value of the iodine index compared to the one for methylene blue indicated a microporous structure of carbon. The presence of iron in this carbon confirms the insertion of ferrous ions during the activation and pyrolysis steps but the low iron content depends on the low concentration of iron solution used for the activation. All these characteristics of FAC were listed from previous work (SANOU *et al.*, 2017).

3.2 Microstructure of FAC

The energy dispersive spectroscopy spectrum is presented in figure 1. Elemental composition (%, wt/wt) of FAC showed 63.1% of C, 23.9% of O, 10.4% of Si, and 2.6% of Fe.

The high carbon content indicates a carbonaceous structure of FAC. Carbon content is lower in FAC compared to AC (SANOU *et al.*, 2016b). The presence of iron in FAC could be due to the insertion of iron ions from the iron chloride solution used for the activation, indicating the possible existence of iron oxides in FAC.

In figure 2, SEM micrographs of FAC are shown with figures 2a and 2b representing the micrographs at 30x and 500x magnifications, respectively. Figure 2a shows a fine structure of FAC with small pore sizes and round particles while figure 2b indicates the narrowed pores. The white spots in figure 2a would be magnetic iron particles incorporated into the FAC during the steps of the activation and the pyrolysis of the rice husk.

Different functional groups at the surface of FAC are identified in the FT-IR spectrum (Figure 3). The band around 3 407.2 cm^{-1} would be the hydroxyl group of cellulose or hemicellulose. The vibration of the double band around 2 21.83 and 2 853.18 cm^{-1} corresponds to the vibrations of Ca-O and Mg-O bonds. The double bond C=C of lignin vibrates at 1 597.19 cm^{-1} (OUEDRAOGO *et al.*, 2015) and the band around 1 480 cm^{-1} is attributed to the vibration of the Cu-O bond. The band at 1 097.17 cm^{-1} could be the vibration of the C-O or Si-O bond. The band at 808.83 cm^{-1} would be the vibration of the Al-O bond and that at 470.38 cm^{-1} is for the Fe-O bond of the iron oxides (MAITI *et al.*, 2010). The existence of the hydroxyl group, C-O bond and the aromatic C=C double bond suggests the presence of phenols and ether oxides, indicating that the sites active on the surface of FAC are mainly acid sites.

Composition of FAC obtained by XRD analysis is given in table 2 where we note the presence of several oxides at different percentages.

It appears that quartz and calcium oxide are predominant oxides in the FAC with a significant amounts of hematite, tenorite, and alumina. However, the presence of crystalline iron phases such as magnetite ($Fe3O_4$) and hematite (α-Fe2O3) confirmed the insertion of iron ions into the rice husk during impregnation step. Magnetite ($Fe3O_4$) has a ferromagnetic property (MEILLON, 1996; GUEYE, 2015). The different oxides detected by XRD analysis are identifiable with the chemical elements detected using EDS analysis. The magnetic separation which indicates the magnetization content of FAC was determined and calculations revealed a magnetization rate of 3.7% indicating a ferromagnetic property of FAC due to the presence of the magnetite in the composition of the FAC.

3.3 Influence of operating parameters on arsenic removal

3.3.1 Effect of pH

pH is known as an essential factor affecting the adsorption process as it influences the surface charge of the adsorbent (MAHMOOD *et al.*, 2018b). As(V) solutions of pH varying from 3 to 11 were prepared by adjusting with NaOH (0.1 M) and HCl (0.1 M) solutions and the contact time was fixed at 60 min after examination of the preliminary results of the variation of contact time. Figure 4 shows a variation of arsenic removal percentage following different steps: a constant part between pH 3 and 5 followed by an increase between pH 5 and 7 with an optimum at pH 7, indicating a maximum removal of As(V) at pH 7. The maximum removal of As(V) at pH 7 can be explained by the fact that at this pH both the $H_2AsO_4^-$ and $HAsO_4^{2-}$ forms of As(V) are present in aqueous solutions. In addition, this point (pH 7) is close to the pH_{ZPC} of FAC and there is no electrostatic repulsion between arsenates and the quasi-neutral surface of FAC. The maximum arsenic removal at pH 7 is in agreement with previous work using iron impregnated tea as the source of activated carbon (MAHMOOD *et al.*, 2018a). Between pH 7 and 9, there is a clear decrease of arsenic removal from 30.5% to 25%, due to the repulsion between arsenate ions and the negative charge on the FAC surface (pH_{ZPC} = 6.72). There is also the competition between arsenate and hydroxyl ions for the same active sites on the adsorbent surface (LIU *et al.*, 2012). No change in As(V) removing was observed after pH 11. The maximum removal at pH 7 corresponds to an adsorption capacity of 153 $\mu g \cdot g^{-1}$ and pH 7 was used in subsequent experiments. According to

Table 1. **Physico-chemical characteristics of ferromagnetic activated carbon (FAC).**
Tableau 1. ***Caractéristiques physicochimiques du charbon actif ferromagnétique..***

Property	Value or range
pH_{ZPC}	6.72
Brunauer-Emmett-Teller (BET) surface ($m^2 \cdot g^{-1}$)	150
Iodine (I_2) index ($mg \cdot g^{-1}$)	199
Methylene blue (MB) index ($mg \cdot g^{-1}$)	15.4
Iron stability (%)	94.85
Grain size (mm)	0.1-1
Bulk density ($g \cdot mL^{-1}$)	0.42
Moisture content (%)	0.01
Residual porosity (%)	62-63

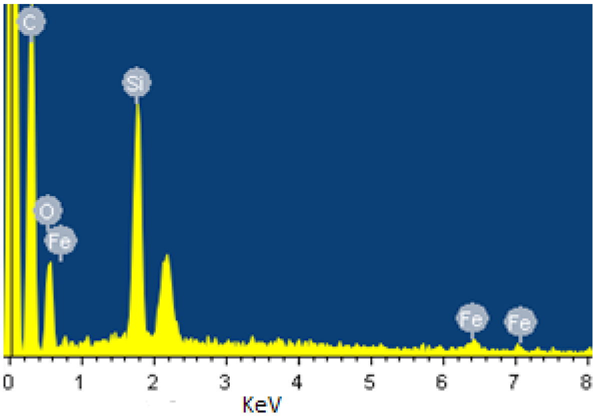

Figure 1. **Energy dispersive spectrum of ferromagnetic activated carbon (FAC).**
Spectre à dispersion d'énergie du charbon actif ferromagnétique.

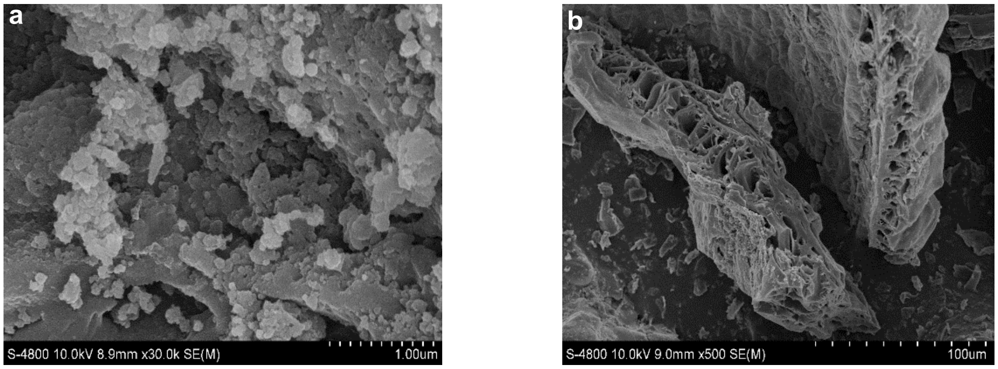

Figure 2. **Scanning electron microscopy image at magnification:s a) 30x, and b) 500x.**
Images par microscopie électronique à balayage à grossissements de : a) 30x et b) 500x.

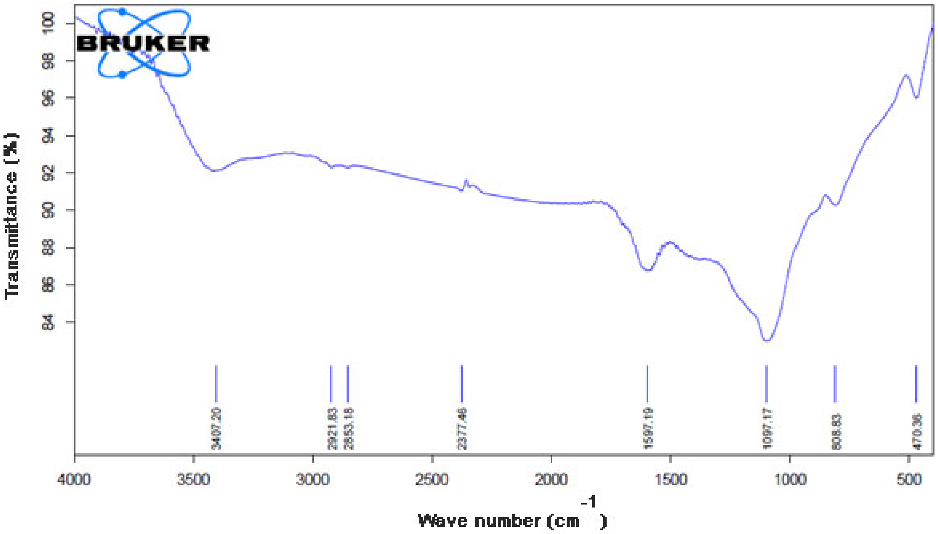

Figure 3. **Fourier transform-infrared spectra of ferromagnetic activated carbon (FAC).**
Spectre infrarouge de la transformée de Fourrier du charbon actif ferromagnétique.

Table 2. Composition of ferromagnetic activated carbon (FAC).
Tableau 2. Composition du charbon actif ferromagnétique.

Oxide	SiO_2	α-Fe_2O_3	Fe_3O_4	Al_2O_3	MgO	CaO	CuO
Content (%, wt/wt)	40.8	9.9	2.8	8.6	4.1	24.3	9.3

the literature, the removal of As(V) using activated carbon occurs by anion exchange process because As(V) has a anionic behavior in aqueous solutions between pH 2 and 12 (ANSARI and SADEGH, 2007).

3.3.2 Effect of initial arsenic concentration

The behavior of As(V) removal was tested with As(V) solutions at concentrations ranging from 200 to 1 000 $\mu g \cdot L^{-1}$, according to arsenic concentration from natural groundwater in Burkina Faso and Vietnam (SANOU *et al.*, 2017). From results (Figure 5), we noticed the decrease in removal from 61% to 30% when the initial concentration of arsenic increased. This result would be due to the fast fixation of arsenate ions combined with a limited number of active sites on the surface of FAC. ANSARI and SADEGH (2007) obtained similar results and they concluded that the lowering of arsenic removal at high concentrations is due to the small number of active sites available on the adsorbent surface. However, arsenic removal capacity increases from 61.6 to 153 $\mu g \cdot g^{-1}$ with initial arsenic concentration between 200 and 800 $\mu g \cdot L^{-1}$ and it remained constant after 800 $\mu g \cdot L^{-1}$ with a maximum capacity of 153 $\mu g \cdot g^{-1}$. The increase of adsorption capacity with initial arsenic concentrations would be due to the increase of arsenate ions and their collision with adsorbent surface (MAHMOOD *et al.*, 2018b)

3.4 Mechanism of As(V) removal

3.4.1 Isotherm models

Three models of isotherms were used with experimental data in order to examine the mechanism of the adsorption process. Data obtained from batch experiments were applied to linearized forms of the isotherm models. The distribution of the adsorbate between the adsorbent surface and the solution at a given temperature can be described by a Langmuir isotherm (Equation 3) and a Freundlich isotherm (Equation 4) (LANGMUIR, 1918; FREUNDLICH, 1906).

$$\frac{C_e}{Q_e} = \frac{1}{Q_m} C_e + \frac{1}{bQ_m} \qquad (3)$$

$$\ln Q_e = \frac{1}{n} \ln C_e + \ln K_F \qquad (4)$$

Figures 6a and 6b represent respectively Langmuir and Freundlich isotherms and the values of the constants are listed in table 3.

Data reported in table 3 showed a high correlation coefficient value (R^2) close to 1 with the calculated capacity of adsorption (q_m) comparable to experimental value (153 $\mu g \cdot g^{-1}$) for the Langmuir isotherm. So, As(V) removal correlated with the Langmuir isotherm indicating a monolayer process. This finding is in agreement with previous studies on arsenic adsorption (MAHMOOD *et al.*, 2018a; MAHMOOD *et al.*, 2018b).

From the Langmuir constant b, free energy of Gibbs can be expressed by following relation (MOHAN and PITTMAN, 2007):

$$\Delta G^{\circ} = -\mathrm{RT} \log b \qquad (5)$$

The calculated value of the Gibbs free energy was 5 $kJ \cdot mol^{-1}$, indicating that the process is not spontaneous but energetically stable on the surface of FAC.

The dimensionless equilibrium parameter R_L indicates if the process is an adsorption or not (HALL *et al.*, 1966). This parameter was calculated using equation 6:

$$R_L = \frac{1}{1 + bC_0} \qquad (6)$$

Values of the dimensionless parameter at equilibrium were ranged between 0 and 1 indicating that As(V) removal was occurred through an adsorption process as indicated in previous work (MAHMOOD *et al.*, 2018a).

It is well known that Langmuir and Freundlich isotherms don't suggest anything about the physical or chemical nature of adsorption. In order to know the nature of adsorption, experimental data were used with the Dubinin-Radushkevich isotherm (SINGH and PANT, 2004).

$$\ln Q_e = \ln Q_m - K\varepsilon^2 \qquad (7)$$

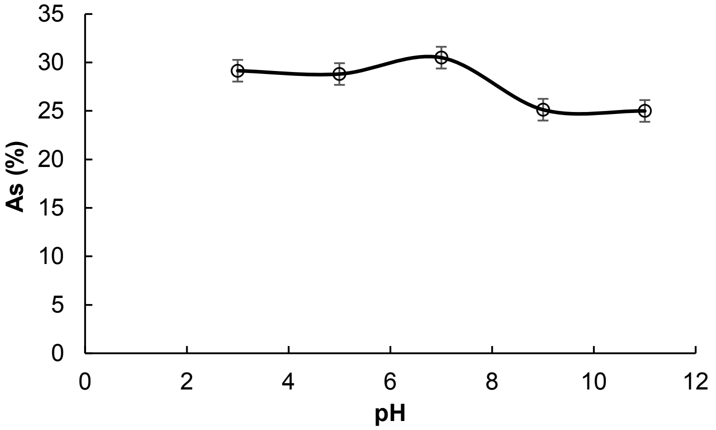

Figure 4. **Effect of pH on As(V) removal with 0.1 g of FAC (ferromagnetic activated carbon), t = 60 min, and C_0 = 1 mg·L^{-1}.**
Effet du pH sur l'élimination de l'As(V) avec 0,1 g de charbon actif ferromagnétique, t = 60 min et C_0 = 1 mg·L^{-1}.

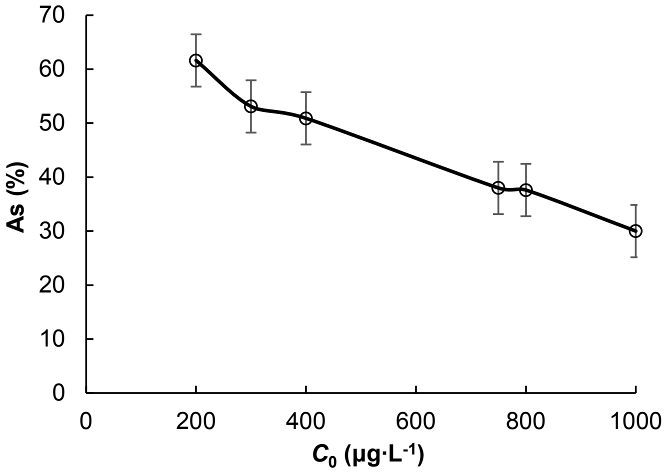

Figure 5. **Effect of initial concentration on As(V) removal with 0.1 g of FAC (ferromagnetic activated carbon) and t = 60 min.**
Effet de la concentration initiale sur l'élimination de l'As(V) avec 0,1 g de charbon actif ferromagnétique et t = 60 min.

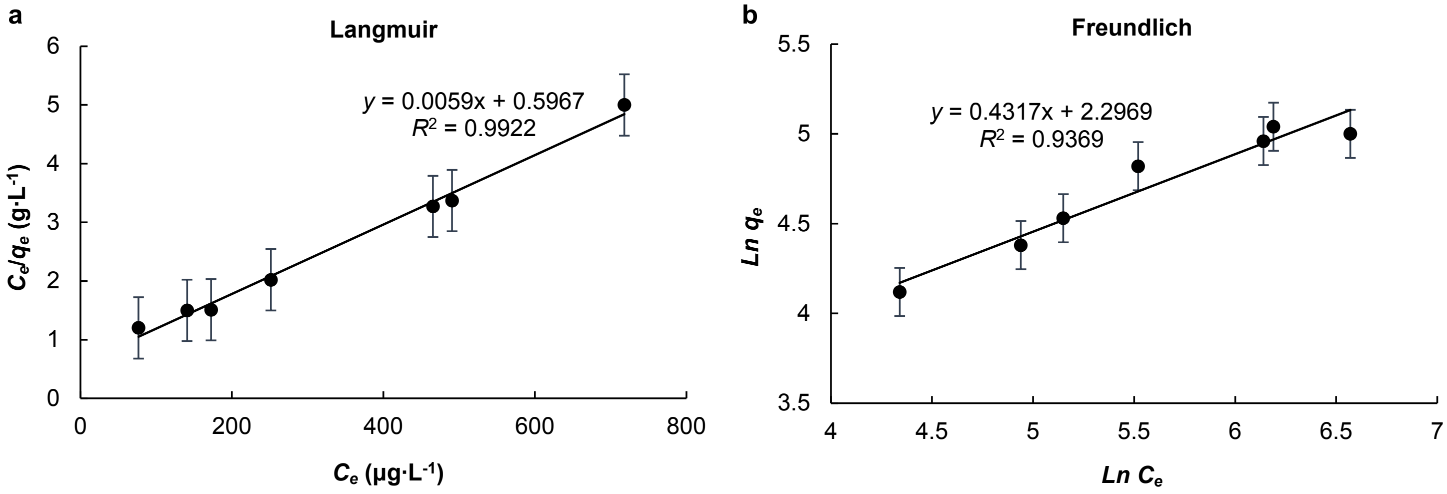

Figure 6. **Plots of a) Langmuir and b) Freundlich isotherms for As(V) removal with 0.1 g of FAC (ferromagnetic activated carbon), t = 60 min, and C_0 = 1 mg·L^{-1}.**
Représentations des isothermes de a) Langmuir et b) Freundlich pour l'élimination de l'As(V) avec 0,1 g de charbon actif ferromagnétique, t = 60 min et C_0=1 mg·L^{-1}

Table 3. **Constants of Langmuir and Freundlich: *b*: thermodynamic equilibrium constant, q_m: maximum adsorption capacity on a monolayer, *n*: affinity of the solute for the adsorbent, K_F : adsorbent ability of the material.**
Tableau 3. ***Constantes de Langmuir et Freundlich : b : constante d'équilibre thermodynamique, q_m : capacité maximale d'adsorption en monocouche, n : affinité du soluté pour l'adsorbant, K_F : pouvoir adsorbant du matériau.***

Langmuir constants			Freundlich constants		
b (L·µg^{-1})	q_m (µg·g^{-1})	R^2	n	K_F (µg·g^{-1})	R^2
0.01	169.5	0.99	2	9.94	0.93

The polanyi potential (ε) can be calculated by the following equation 8:

$$\varepsilon = \mathrm{RT} * \ln(1 + \frac{1}{C_e}) \tag{8}$$

The representation of this isotherm model is given by the figure 7.

The free energy of adsorption (*E*), defined as the free energy change when one mole of ion is transferred from infinity to the surface of solid in the solution, was calculated as well (MAJI *et al.*, 2008).

$$E = (2K)^{-0.5} \tag{9}$$

The value of adsorption energy was 14.14 kJ·mol^{-1} (Table 4); this value between 8 and 16 kJ·mol^{-1} indicates an ion exchange process (HAN *et al.*, 2013), presumably an anion exchange between arsenates and hydroxyl ions involving covalent bonds between arsenates and active sites on the surface. This process, which is seen as the beginning of chemisorption, lends to the formation of inner sphere complexes. This result is in agreement with previous works using activated carbon which suggested physico-chemical adsorption (ANSARI and SADEGH, 2007). We can conclude that both adsorption and anion exchange constitute the mechanism of As(V) removal as a monolayer, as indicated in the literature (RAUL *et al.*, 2013; SHAHID *et al.*, 2019).

3.4.2 Kinetic studies

3.4.2.1 Effect of contact time on As(V) removal

The contact time is an important parameter in batch experiments. From figure 8, the percentage of arsenic removal increased from 24.2% to 48% as the contact time increased from 5 to 120 min, following two steps. The first step between 5 and 60 min corresponded to the gradual occupation of different active sites on the FAC. The increasing phase would be the result of the formation of stronger complex or the migration of arsenates onto the surface of the carbon (SU and PULS, 2001). After 60 min (second step), no change in arsenic removal was observed. This can be explained by the saturation of active sites or the limited number of micropores on the surface of FAC. At saturation, the maximum adsorption capacity of FAC was 153 µg·g^{-1} of FAC after 60 min of contact. However, the arsenic removal capacity of FAC remains lower compared to GFH (8 500 µg·g^{-1}) under similar conditions (DRIEHAUS *et al.*, 1998). The two-step process of arsenic sorption onto FAC may be due to the involvement of a fast ion exchange process followed by chemisorption (MAHMOOD *et al.*, 2011).The initial rapid adsorption rate is perhaps the result of the accessibility of arsenate anions in solution to abundant sites on the surface. However, arsenate ions were adsorbed competitively in the following minutes due to the limited availability of surface sites (DIN *et al.*, 2017).

3.4.2.2 Kinetic models

In order to understand the mechanism of As(V) adsorption, the kinetic data were analyzed using kinetic models. There are the pseudo-first order from equation of LAGERGREN and SVENSKA (1898) based on the adsorption capacity (Equation 10) and pseudo-second order from equation of HO and MCKAY (1999) based on the equilibrium between adsorbate and adsorbent (Equation 11).

$$\ln(Q_e - Q_t) = -K_1 t + \ln Q_e \tag{10}$$

$$\frac{t}{Q_t} = \frac{1}{Q_e} t + \frac{1}{K_2 Q_e^2} \tag{11}$$

with equation (10) representing the pseudo-first order model and equation (11) the pseudo-second order model.

The representation of these equations has given the graphs in figure 9 and the constants of the models are listed in table 5.

A higher value of the correlation coefficient (R^2) close to 1 was found with the pseudo-second order model compared to the pseudo-first order model. In addition, the theoretical value of the adsorption capacity q_{theo} (238 µg·g^{-1}) was comparable (close) to the experimental value q_{exp} (240 µg·g^{-1}) using the pseudo-second-order model. These results indicate that the removal of As(V) occurred following pseudo-second order kinetics with a kinetic constant of 0.003 g·µg^{-1}·min^{-1}. This result is confirmed by literature data on the kinetic studies of arsenic removal (DIN *et al.*, 2017; ANSONE *et al.*, 2012).

It is generally known that the sorption process is a rate-controlled process, in which the slowest step determines the process rate-limiting step. The kinetic data were further analyzed assuming that the mechanism of soil sorption can generally be described by four consecutive rate-controlling steps, which are external mass transfer, film diffusion, intraparticle diffusion, and surface interactions on active sites (HO *et al.*, 2000; OCAMPO-PEREZ *et al.*, 2012). The rate-limiting step of the sorption can be qualitatively determined by analyzing kinetic data using the Weber-Morris model (WEBER and MORRIS, 1963; OFOMAJA, 2010):

$$Q_e = K_i t^{0.5} + C \tag{12}$$

where, K_i is the diffusion coefficient (µg·g^{-1}·min$^{-0.5}$) and *C* is a constant that gives an indication of the thickness of boundary layer. The sorption process is said to be intraparticle diffusion controlled, if the straight line plot passes through the origin, while the boundary layer diffusion (external mass transfer or

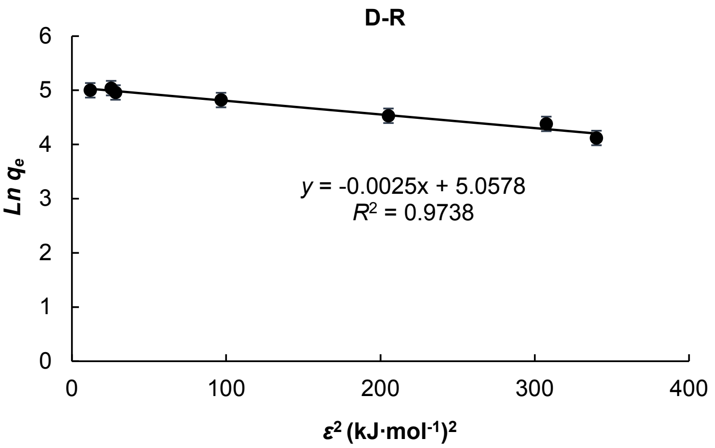

Figure 7. **Dubinin-Radushkevich isotherm plot for As(V) removal with 0.1 g of FAC (ferromagnetic activated carbon), t = 60 min, and C_0 = 1 mg·L^{-1}.**
Représentation de l'isotherme de Dubinin-Radushkevich pour l'élimination de l'As(V) avec 0,1 g de charbon actif ferromagnétique, t = 60 min et C_0=1 mg·L^{-1}

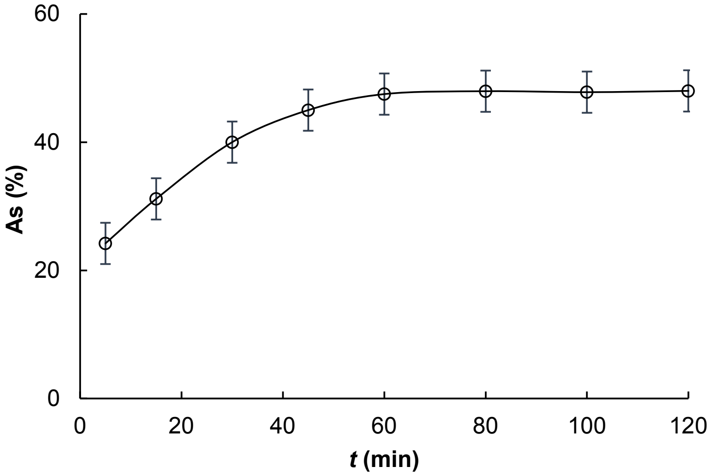

Figure 8. **Effect of contact time on As(V) removal with 0.1 g of FAC (ferromagnetic activated carbon), pH = 3.6, and C_0 = 1 mg·L^{-1}.**
Effet du temps de contact sur l'élimination de l'As(V) avec 0,1 g de charbon actif ferromagnétique, pH = 3,6 et C_0=1 mg·L^{-1}.

Table 4. **Constants of Dubinin-Radushkevich isotherm: q_m: maximum adsorption capacity, K: adsorption constant linked to the free energy of the adsorption (E).**
Tableau 4. Constantes de l'isotherme de Dubinin-Radushkevich : q_m : capacité maximale d'adsorption, K : constante d'adsorption liée à l'énergie libre d'adsorption (E).

q_m (mg·g^{-1})	K (mol^2·kJ^{-2})	R^2	E (kJ·mol^{-1})
0.157	0.005	0.97	14.14

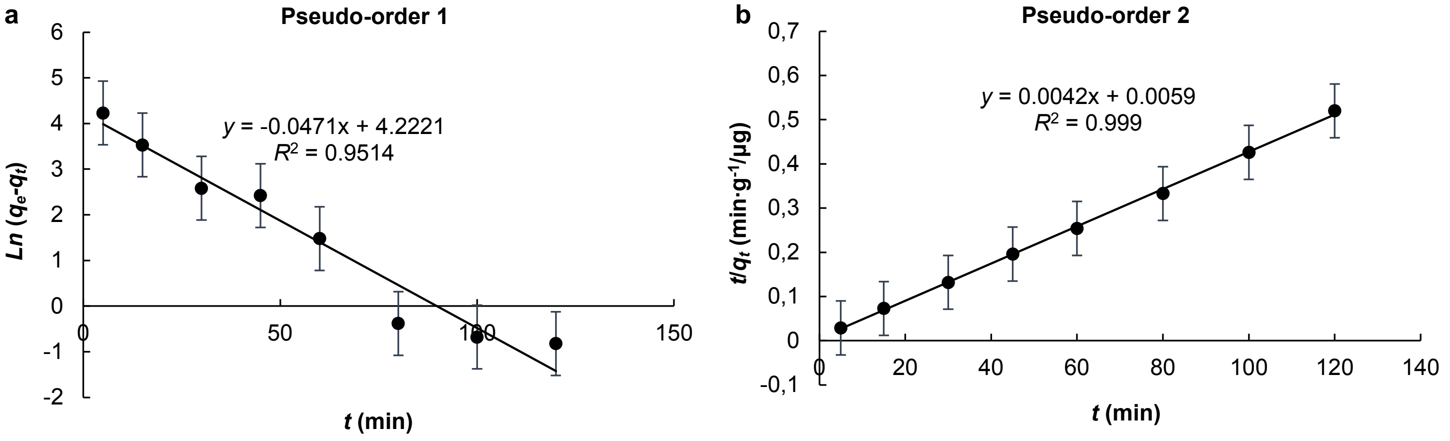

Figure 9. **Plots of a) pseudo-first, and b) pseudo-second order kinetic model for As(V) removal with 0.1 g of FAC (ferromagnetic activated carbon) and C_0 = 1 mg·L^{-1}.**
Représentations des modèles cinétiques de a) pseudo-premier et b) pseudo-second ordre pour l'élimination de l'As(V) avec 0,1 g de charbon actif ferromagnétique et C_0=1 mg·L^{-1}.

Table 5. Constants of pseudo-first and pseudo-second order kinetic models: *K*: kinetic constant (speed constant for pseudo-order 1 and kinetic rate for pseudo-order 2), q_{theo}: theoretical adsorption capacity, q_{exp}: experimental adsorption capacity.

Tableau 5. Constantes des modèles cinétiques de pseudo-premier et pseudo-second ordres : K : constante cinétique (constante de vitesse pour le pseudo-premier ordre et taux cinétique pour le pseudo-second ordre), q_{theo} : capacité d'adsorption théorique, q_{exp} : capacité d'adsorption expérimentale.

Reaction order	*K* (min^{-1})	q_{theo} (µg·g^{-1})	q_{exp} (µg·g^{-1})	R^2
Pseudo-order 1	0.047	68.17	240	0.95
Pseudo-order 2	0.003	238.10	240	0.99

film diffusion) may take place if it does not pass through the origin (HO *et al.*, 2000). The plot representing this kinetic model is given in the figure 10.

The calculations revealed the correlation coefficient value of 0.75, and the constant K_i of 5.66 µg·g^{-1}·min^{-1}. The low value of R^2 and the observation that the curve doesn't pass through the origin indicate that the intraparticle diffusion is not the limiting step of the process and the mechanism of the process is complex. However, the high value of intercept *C* (182.43) indicates the effect of transboundary layer. We conclude that the process of As(V) adsorption is controlled by film diffusion as described in the literature (HO *et al.*, 2000; MAHMOOD *et al.*, 2018b; DIN *et al.*, 2017).

3.5 Comparison of adsorption capacity

The comparison of the adsorption capacity of FAC with other adsorbents is a challenge because of the differences in experimental conditions, which impact considerably on the adsorption capacities. However, for the sake of comparison, the values of monolayer adsorption capacity (q_m) collected from the literature for various adsorbents under the similar conditions and the one for ferromagnetic activated carbon in the present study are listed in table 6.

The comparison of adsorption capacities (Table 6) indicates that the FAC has an adsorption capacity (153 µg·g^{-1}) greater than that of ferrihydrite and iron oxide coated sand used as adsorbents (THIRUNAVUKKARASU *et al.*, 2003; MOHAN and PITTMAN, 2007). However, this capacity remains lower compare to GFH and iron-coated materials previously studied (DRIEHAUS *et al.*, 1998; TAWABINI *et al.*, 2011; PEHLIVAN *et al.*, 2013). In addition, the adsorption capacity of materials such as laterite soil and ash remains lower than that for the ferromagnetic activated carbon used in the present work (NEMADE *et al.*, 2009, MAITI *et al.*, 2007, MOSTAFAPOUR *et al.*, 2013). This comparison cannot be more exact because of some experimental factors such as pH, nature of water or solution, temperature, adsorbent weight, etc.).

We conclude that, FAC is a promising adsorbent for the removal of As(V) under the prescribed conditions, compared to other adsorbents.

4. CONCLUSION

Activated carbon (AC) prepared from rice husk and iron chloride solution was effectively a carbonaceous material with an iron content of 2.6% and a magnetization content of 3.7%. X-ray diffraction showed that the magnetite is the oxide responsible of the ferromagnetic property of FAC. Results from batch experiments indicate that this carbon is an effective adsorbent for As(V) removal from water. The variations of pH revealed an optimum removal of As(V) at pH 7 corresponding to an adsorption capacity of 153 µg·g^{-1} for 60 min of contact time. The removal percentage decreased with the increase of initial arsenic concentration while the adsorption capacity of FAC from calculations increased from 61.62 to 153 µg·g^{-1}. The increase of the contact time caused an increase of the removal percentage until the saturation of all active sites on the surface of FAC after 60 min of contact, corresponding to the maximum capacity of 153 µg·g^{-1}. The study of the isotherm models revealed a process correlated with the Langmuir isotherm, indicating a monolayer adsorption. The value of free energy of adsorption indicated an anion exchange between arsenates and hydroxyl ions. The removal of As(V) using FAC occurred following a mechanism including both adsorption and ion-exchange with pseudo-second order kinetics. Consequently, this material could be used as a fixed bed in column experiments and pilot systems for the removal of arsenic using real groundwaters.

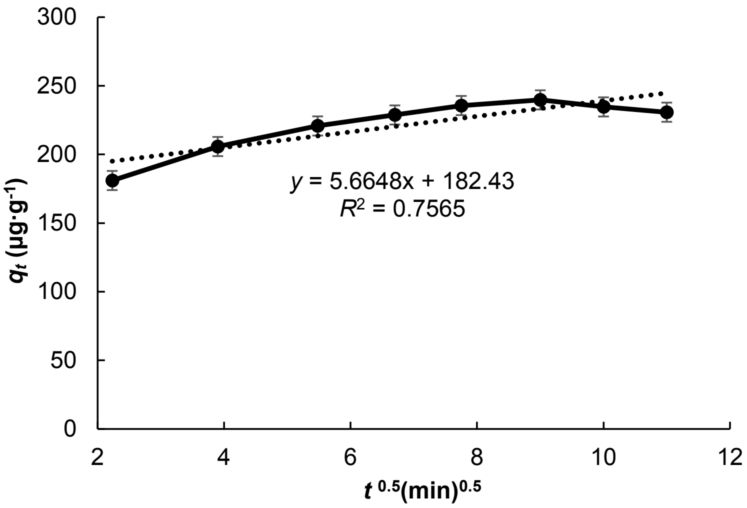

Figure 10. **Kinetic model of intraparticle diffusion for As(V) removal with 0.1 g of FAC (ferromagnetic activated carbon), C_0 = 1 mg·L^{-1}, and T = 26 ± 2°C.**
Modèle cinétique de la diffusion intraparticulaire pour l'élimination de l'As(V) avec 0,1 g de de charbon actif ferromagnétique, C_0 = 1 mg·L^{-1} et T = 26 ± 2 °C.

Table 6. **Comparison of adsorption capacity of ferromagnetic activated carbon (FAC) with other adsorbent materials.**
Tableau 6. ***Comparaison de la capacité d'adsorption du charbon actif ferromagnétique avec d'autres adsorbants.***

Adsorbent	Type of water	pH	Surface area (m²·g⁻¹)	Temperature (°C)	Adsorption capacity (mg·g⁻¹)		Reference
					As(III)	As(V)	
Iron oxide-coated sand (IOCS)	Tap	–	–	22 ± 2	0.136	–	THIRUNAVUKKARASU *et al.* (2005)
	Drinking	7.6	10.6	22 ± 2	0.041	0.043	THIRUNAVUKKARASU *et al.* (2003)
Ferrihydrite	Natural	–	141	–	–	0.025	MOHAN AND PITTMAN Jr. (2007)
Granular ferric hydroxide (GFH)	Aqueous solutions	3	240	26 ± 2	–	0.10	SANOU *et al.* (2016a)
	Natural water	7	–	–	Total As 8.5		DRIEHAUS *et al.* (1998)
Ferromagnetic activated carbon (FAC)	Aqueous solutions	7	150	26 ± 2	–	0.153	Present study
Ferric ion-loaded red mud	–	7	–	25	4	–	TAWABINI *et al.* (2011)
Iron-coated rice husk	Aqueous solutions	4	–	22 ± 2	–	2.5	PEHLIVAN *et al.* (2013)
Iron-used tea activated carbon	Aqueous solutions	8	165	25	6.83	–	MAHMOOD *et al.* (2018a)
Laterite soil	Aqueous solutions	7.2	16.05	17	0.086	–	NEMADE *et al.* (2009)
		7.2	18.05	29	0.17	–	MAITI *et al.* (2007)
Salvadora persica stem ash	Aqueous solutions	6	–	27	–	0.004	MOSTAFAPOUR *et al.* (2013)

ACKNOWLEDGEMENTS

Authors are thankful to Federal Ministry for Economic Cooperation and Development, Germany (BMZ), German Academic Exchange Service (DAAD), Excellence Center for Development Cooperation, Sustainable Water Management (EXCEED/SWINDON), and Technical University of Braunschweig (TUBS) for their financial and technical supports.

REFERENCES

ANSARI R. and M. SADEGH (2007). Application of activated carbon for removal of arsenic ions from aqueous solutions. *E-J. Chem.*, 4, 103-108.

ANSONE L., M. KLAVINS, A. ROBALDS and A. VIKSNA (2012). Use of biomass for removal of arsenic compounds. *Latvian J. Chem.*, 4, 324-335.

BERG M., H.C. TRAN, T.C. NGUYEN, H.V. PHAM, R. SCHERTENLEIB and W. GIGER (2001). Arsenic contamination of groundwater and drinking water in Vietnam: a human health threat. *Environ. Sci. Technol.*, 35, 2621-2626.

DESJARDINS R. (1997). *Le traitement des eaux.* 2^{e} édition, École polytechnique de Montréal (QC), Canada, 303 p.

DIN S.U., T. MAHMOOD, A. NAEEM, M. HAMAYUN and N.S. SHAH (2017). Detailed kinetics study of arsenate adsorption by a sequentially precipitated binary oxide of iron and silicon. *Environ. Technol.*, 40, 261-269.

DRIEHAUS W., M. JEKEL and U. HILDEBRANDT (1998). Granular ferric hydroxide - a new adsorbent for the removal of arsenic from natural water. *J. Water Supply Res. T.*, 47, 30-35.

FREUNDLICH H.M.F. (1906). Über die Adsorption in Lösungen. *Zeitschrift für Physikalische Chemie*, 57, 385-470.

GUEYE M. (2015). *Développement de charbon actif à partir de biomasses lignocellulosiques pour des applications dans le traitement de l'eau.* Thèse de doctorat, Institut International de l'Ingénierie de l'Eau et de l'Environnement (2iE), Burkina Faso, 229 p.

HALL K.R., L.C. EAGLETON, A. ACRIVOS and T. VERMEULEN (1966). Pore and solid-diffusion kinetics in fixed-bed adsorption under constant-pattern conditions. *Indus. Eng. Chem. Fund. J.*, 5, 212-223.

HAN C., H. LI, H. PU, H. YU, L. DENG, S. HUANG and Y. LUO (2013). Synthesis and characterization of mesoporous alumina and their performances for removing arsenic (V). *Chem. Eng. J.*, 217, 1-9.

HO Y.S. and G. MCKAY (1999). Pseudo second order model for sorption process. *Process Biochem.*, 34, 451-465.

HO Y.S., J.C.Y. NG and G. MCKAY (2000). Kinetics of pollutant sorption by biosorbents: review. *Sep. Purif. Rev.*, 29, 189-232.

HUGHES M.F. (2002). Arsenic toxicity and potential mechanisms of action. *Toxicol. Lett.*, 133, 1-16.

KNUDSEN J., Y. PRADELLES and A. ZOUGOURI (2005). *Étude approfondie dans 8 villages de la région Nord ayant des forages à taux d'arsenic élevés.* Projet DANIDA, Ministère des Affaires étrangères, Burkina Faso, pp. 6-98.

LAGERGREN S. and B.K. SVENSKA (1898). About the theory of so-called adsorption of soluble substances. *Kungliga Svenska Vetenskapsakademiens Handlingar*, 24, 1-39.

LANGMUIR I. (1918). The adsorption of gases on plane surfaces of glass, mica and platinum. *J. Am. Chem. Soc.*, 40, 1361-1403.

LIU X., H. AO, X. XIONG, J. XIAO et J. LIU (2012). Arsenic removal from water by iron-modified bamboo charcoal. *Water Air Soil Pollut.*, 223, 1033-1044.

MAHMOOD T, T. SADDIQUE, A. NAEEM, M. ASLAM and R. ALI (2011). Kinetic and thermodynamic study of Cd(II), Co(II) and Zn(II) adsorption from aqueous solution by NiO. *Chem. Eng. J.*, 171, 935-940.

MAHMOOD T., M. ASLAM, A. NAEEM, T. SIDDIQUE and S. UD DIN (2018a). Adsorption of As(III) from aqueous solutions onto iron impregnated used tea activated carbon: Equilibrium, kinetic and thermodynamic study. *J. Chil. Chem. Soc.*, 63, 3855-3866.

MAHMOOD T., M. ASLAM, A. NAEEM, R. ALI and T. SADDIQUE (2018b). Equilibrium, kinetics, mechanism and thermodynamics studies of As(III) adsorption from aqueous solution using iron impregnated used tea. *Desalin. Water Treat.*, 104, 135-148.

MAITI A., S. DASGUPTA, J.K. BASU and S. DE (2007). Adsorption of arsenite using natural laterite as adsorbent. *Sep. Purif. Technol.*, 55, 350-359.

MAITI A., J.K. BASSU and S. DE (2010). Development of a treated laterite for arsenic adsorption: Effects of treatment parameters. *Ind. Eng. Chem. Res.*, 49, 4873-4886.

MAJI S.K., A. PAL, T. PAL and A. ADAK (2007). Modeling and fixed bed column adsorption of As (III) on laterite soil. *Sep. Purif. Technol.*, 56, 284-290.

MAJI S.K., A. PAL and T. PAL (2008). Arsenic removal from real-life ground water by adsorption on laterite soil. *J. Hazard. Mater.*, 151, 811-820.

MEILLON S. (1996). *Étude des nouvelles propriétés de la magnétite et de l'hématite après transformation par irradiation et par mécanosynthèse.* Thèse de doctorat, Univ. Paris XI Orsay, Univ. Paris Sud, France, 224 p.

MEROLA R.B., T.T. HIEN, D.T.T. QUYEN and A. VENGOSH (2015). Arsenic exposure to drinking water in the Mekong delta. *Sci. Total Environ.*, 511, 544-552.

MOHAN D. Jr. and C.U. PITTMAN (2007) Arsenic removal from water/wastewater using adsorbents: a critical review. *J. Hazard. Mater.*, 142, 1-53.

MOSTAFAPOUR F.K., E. BAZRAFSHAN, M. FARZADKIA and S. AMINI (2013). Arsenic removal from aqueous solutions by *Salvadora persica* stem ash. *J. Chem.*, 2013, 1-8.

NEMADE P.D., A.M. KADAM and H.S. SHANKAR (2009). Adsorption of arsenic from aqueous solution on naturally available red soil. *J. Environ. Biol.*, 30, 499-504.

OCAMPO-PEREZ R., M.M. ABDEL DAIEM, J. RIVERA-UTRILLA, J.D. MENDEZ-DIAZ and M. SANCHEZ-POLO (2012). Modeling adsorption rate of organic micropollutants present in landfill leachates onto granular activated carbon. *J. Colloid Interface Sci.*, 385, 174-182.

OFOMAJA A.E. (2010). Intraparticle diffusion process for lead (II) biosorption onto mansonia wood sawdust. *Biores. Technol.*, 101, 5868-5876.

OUEDRAOGO W.K.I., E. PEHLIVAN, H. TRAN, L.Y. BONZI-COULIBALY, D. ZACHMANN, and M. BAHADIR (2015). Synthesis of iron hydroxide-coated rice straw (IOC-RS) and its application in arsenic (V) removal from water. *J. Water Health.*, 13, 726-736.

PEHLIVAN E., T.H. TRAN, W.K.I. OUEDRAOGO, C. SCHMIDT, D. ZACHMANN and M. BAHADIR (2013). Removal of As(V) from aqueous solutions by iron-coated rice husk. *Fuel Process. Technol.*, 106, 511-517.

RAUL P.K., R.R. DEVI, I.M. UMLONG, A.J. THAKUR, S. BANERJEE and V. VEER (2013). Iron oxide hydroxide nanoflower assisted removal of arsenic from water. *Mater. Res. Bull.*, 49, 360-368.

SANOU Y., S. PARE, N.T.T. PHUONG and N.V. PHUOC (2016a). Experimental and kinetic modelling of As(V) adsorption on Granular Ferric Hydroxide and laterite. *J. Environ. Treat. Tech.*, 4, 62-70.

SANOU Y., S. PARE, G. BABA, N.K. SEGBEAYA and L.Y. BONZI-COULIBALY (2016b). Removal of COD in wastewaters by activated charcoal from rice husk. *J. Water Sci.*, 29, 265-277.

SANOU Y., S. PARE, N.T.T. PHUONG and N.V. PHUOC (2017). Arsenic removal from groundwater using filtering through Ferromagnetic Carbon. *Proceedings of the Experts Workshop*, Cuvillier Publisher Verlag Göttingen, Germany, pp. 93-103.

SHAHID M.K., P. SAN and Y.G. CHOI (2019). Evaluation of arsenate adsorption efficiency of mill-scale derived magnetite particles with column and plug flow reactors. *J. Water Process Eng.*, 28, 260-268.

SHANKAR S. and U. SHANKER (2014). Arsenic contamination of groundwater: A review of sources, prevalence, health risks, and strategies for mitigation. *Sci. World J.*, 2014, 1-18.

SINGH T.S. and K.K. PANT (2004). Equilibrium, kinetics and thermodynamic studies for adsorption of As (III) on activated alumina. *Sep. Purif. Technol.*, 36, 139-147.

SMEDLEY P.L., J. KNUDSEN and D. MAIGA (2007). Arsenic in groundwater from mineralized Proterozoic basement rocks of Burkina Faso. *Appl. Geochem.*, 22, 1074-1092.

SOME I.T., A.K. SAKIRA, M. OUEDRAOGO, T.Z. OUEDRAOAGO, A. TRAORE, B. SONDO and P.I. GUISSOU (2012). Arsenic levels in tube-wells water, food, residents' urine and the prevalence of skin lesions in Yatenga Province, Burkina Faso. *Interdiscip. Toxicol.*, 5, 38-41.

SU C. and R. PULS (2001). Arsenate and arsenite removal by zerovalent iron: Kinetics, redox transformation, and implications for *in situ* groundwater remediation. *Environ. Sci. Technol.*, 35, 1487-1492.

TAWABINI B.S., S.F.A. AL-KHALDI, M.M. KHALED and M.A. ATIEH (2011). Removal of arsenic from water by iron oxide nanoparticles impregnated on carbon nanotubes. *J. Environ. Sci. Health A*, 46, 215-223.

THAJEEL A.S., A.Z. RAHEEM and M.M. AL-FAIZE (2013). Production of activated carbon from local raw materials using physical and chemical preparation methods. *J. Chem. Pharm. Res.*, 5, 251-259.

THIRUNAVUKKARASU O.S., T. VIRARAGHAVAN and K.S. SUBRAMANIAN (2003). Arsenic removal from drinking water using iron-oxide coated sand. *Water Air Soil Pollut.*, 142, 95-111.

THIRUNAVUKKARASU O.S., T. VIRARAGHAVAN, K.S. SUBRAMANIAN, O. CHAALAL and M.R. ISLAM (2005). Arsenic removal in drinking water: impacts and novel removal technologies. *Energy Sources*, 27, 209-219.

US ENVIRONMENTAL PROTECTION AGENCY (USEPA) (2001). *National primary drinking-water regulations: Arsenic and clarifications to compliance and new source contaminants monitoring*. US Environmental Protection Agency, US Code of Federal Regulations, 66 FR 6975, pp. 6976-7066.

WEBER W.J. and J.C. MORRIS (1963). Kinetics of adsorption on carbon from solution. *J. Sanit. Eng. Div. ASCE*, 89, 31-60.